Atmos. Chem. Phys. Discuss., 12, 21399–21435, 2012
www.atmos-chem-phys-discuss.net/12/21399/2012/
doi:10.5194/acpd-12-21399-2012

Atmospheric Chemistry and Physics Discussions

Influence of biomass burning and anthropogenic emissions on ozone, carbon monoxide and black carbon concentrations at the Mt. Cimone GAW-WMO global station (Italy, 2165 m a.s.l.)

P. Cristofanelli[1], F. Fierli[1], A. Marinoni[1], R. Duchi[1], J. Burkhart[2], A. Stohl[2], M. Maione[3], J. Arduini[3], and P. Bonasoni[1]

[1]National Research Council of Italy – Institute of Atmospheric Sciences and Climate, Bologna, Italy
[2]NILU – Norwegian Institute for Air Research, Kjeller, Norway
[3]University of Urbino "Carlo Bo" – Dipartimento di Scienze di Base e Fondamenti, Urbino, Italy

Received: 15 June 2012 – Accepted: 7 August 2012 – Published: 21 August 2012

Correspondence to: P. Cristofanelli (p.cristofanelli@isac.cnr.it)

Published by Copernicus Publications on behalf of the European Geosciences Union.

ACPD

12, 21399–21435, 2012

Abstract

This work investigates the variability of ozone (O_3), carbon monoxide (CO) and equivalent black carbon (BC) concentrations at the Italian Climate Observatory "O. Vittori" (ICO-OV), part of the Mt. Cimone global GAW-WMO station (Italy). For this purpose, ICO-OV observations carried out in the period January 2007–June 2009, have been analysed and correlated with the output of the FLEXPART Lagrangian dispersion model to specifically evaluate the influence of biomass burning (BB) and anthropogenic emissions younger than 20 days. During the investigation period, the average O_3, CO and BC concentrations at ICO-OV were 54 ± 3 ppbv, 122 ± 7 ppbv and 213 ± 34 ng m^{-3} (mean ± expanded uncertainty with $p < 95\,\%$), with clear seasonal cycles characterized by summer maxima and winter minima for O_3 and BC and spring maximum and summer minimum for CO.

According to FLEXPART output, BB impact is maximized during the warm months from July to September but appeared to have a significant contribution to the observed tracer concentrations only during specific transport events. We characterised in detail five major events with respect to transport scales (i.e. global, regional and local), source regions and O_3, CO and BC variations. For these events, very large variability of enhancement ratios O_3/CO (from −0.22 to 0.71) and BC/CO (from 2.69 to 29.83 ng m^{-3} ppbv^{-1}) were observed.

CO related with anthropogenic emissions (CO_{ant}) contributed to 17.4 % of the mean CO value observed at ICO-OV, with the warm months appearing particularly affected by transport events of air-masses rich in anthropogenic pollution. The proportion of tracer variability that is described by FLEXPART CO_{ant} peaked to 37 % (in May–September) for CO, 19 % (in May–September) for O_3 and 32 % (in January–April) for BC. During May–September, the analysis of the correlation among CO, O_3 and BC as a function of the CO_{ant} indicated that ICO-OV was influenced by air-masses rich in anthropogenic pollution transported from the regional to the global scale. On the other side, CO and O_3 were negatively correlated during October–December, when FLEXPART does not

ACPD
12, 21399–21435, 2012

show significant presence of recent anthropogenic emissions and only a few observations are characterized by enhanced BC. Such behaviour may be attributed to an ensemble of processes concurrent in enhancing O_3 with low CO (upper troposphere/lower stratosphere intrusions) and O_3 titration by NO in polluted air-masses along with lower photochemical activity. An intermediate situation occurs in January–April when CO and O_3 were almost uncorrelated and BC enhancements were associated to relatively old (10 days) anthropogenic emissions.

1 Introduction

Tropospheric carbon monoxide (CO), ozone (O_3) and black carbon (BC) have a substantial impact on climate and air quality. CO, primarily emitted from combustion processes (also formed in substantial amounts from methane oxidation), strongly influences the abundance of the OH radical and thereby alters the lifetime of methane and other greenhouse gases (e.g. Seinfeld and Pandis, 1998; Forster et al., 2007). O_3 is involved in photochemical reactions (e.g. Crutzen et al., 1999; Volz-Thomas et al., 2002) and in determining the overall oxidation capacity of the troposphere (Gauss et al., 2003). Moreover, it is a harmful pollutant (Conti et al., 2005) and an efficient greenhouse gas (Forster et al., 2007). Due to its direct impact on solar and thermal radiation, BC was recognised as an important factor contributing to global warming (Andreae and Gelencsér, 2006 and references therein). Additionally, BC causes an indirect radiative forcing by modifying the concentration and size spectrum of cloud droplets (e.g. Lohmann et al., 2000; Forster et al., 2007) and it decreases the surface albedo of snow (e.g. Flanner et al., 2009).

Southern Europe and the Mediterranean basin (hereafter SE/MB) are recognised as a hot-spot region both in terms of climate change (e.g. Forster et al., 2007) and air-quality (Monks et al., 2009), also representing a major crossroad of different air mass transport processes (Lelieveld et al., 2002; Millàn et al., 2006; Duncan et al., 2008). The transport of polluted air masses from Europe and other continents can influence

ACPD
12, 21399–21435, 2012

the variability of trace gases and aerosol over SE/MB. In particular, large amounts of anthropogenic pollutants emitted in continental Europe are transported towards the SE/MB especially during summer (e.g. Duncan et al., 2008; Henne et al., 2004, 2005), when intense photochemical O_3 production also occurs (see for instance; Vautard et al., 2005). Moreover, in the past decade many studies have revealed significant intercontinental transport of air-masses rich in anthropogenic pollutants or biomass burning emissions from North America to Europe (e.g. Stohl and Trickl, 1999; Stohl et al., 2003, Auvray and Bay, 2005; Huntrieser et al., 2005). In particular, biomass burning (BB) represents a major source of atmospheric pollutants and climate altering species (e.g. Crutzen and Andreae, 1990; Simmonds et al., 2005) and forest wildfires have a considerable impact on the variability of CO, O_3 and BC in the Northern Hemisphere (e.g. Novelli et al., 2003; van der Werf et al., 2006; Bond et al., 2011). BC produced by boreal wildfires accounts for 10 % of the annual anthropogenic BC emissions in the Northern Hemisphere (Bond et al., 2004). Previous studies have shown that the atmospheric compounds directly emitted by BB or produced by photochemical processes occurring within BB plumes can be transported over long distances, thus affecting both air quality and climate from local to global scales (e.g. Val Martin et al., 2006 and references therein). SE/MB can also be affected by large wildfire events in Europe, especially during summer (e.g. Pace et al., 2006; Cristofanelli et al., 2007; Turquety et al., 2009).

The pollutant budget in the Mediterranean basin may also vary due to climate change. A dryer and warmer climate in the Mediterranean region, as projected by climate models, can lead both to an increase in pollution sources such as wildfire events and to enhanced photochemical O_3 production (Solomon et al., 2007) with a dramatic change in pollutants transport pattern over Europe (Forster et al., 2007).

In this work, we quantify the variability of O_3, CO and BC over SE/MB from daily to seasonal timescales: observations are acquired on a routine basis at the Italian Climate Observatory "O. Vittori" (ICO-OV) of the Mt. Cimone global GAW-WMO station (CMN, 44°11′ N, 10°42′ E, 2165 m a.s.l.) during the period 2007–2009. The ICO-OV lo-

ACPD
12, 21399–21435, 2012

cation is considered representative for the baseline conditions of the Mediterranean free troposphere (Bonasoni et al., 2000; Fischer et al., 2003) and only during the warm months an influence of air-mass transport from the regional boundary layer is detected due to convective processes and breeze regimes (Fischer et al., 2003; Van Dingenen, 2005). Three years of observations are analyzed here to identify the role of BB (as done in Cristofanelli et al., 2009 for a specific event) and anthropogenic pollution transport to the observed compound variability. The Lagrangian atmospheric transport model FLEXPART provides an estimate of the emission age of BB and anthropogenic emissions at ICO-OV and, coupled to the observations, can allow to quantify the roles played by these emission types to the atmospheric composition variability.

2 Experimental and methodologies

2.1 Observations

At the ICO-OV, tropospheric O_3 measurements have been carried out continuously since 1996 using a UV-photometric analyser (Dasibi 1108). The accuracy and quality of measurements (sampling time: 1 min, combined standard uncertainty less than ±2 ppbv in the range 1–100 ppbv) and sampling procedures are guaranteed within the GAW requirements (WMO, 2002). In particular, the O_3 analyser working at ICO-OV was traced back to SRP#15 Standard Reference Photometer at EMPA (Swiss Federal Laboratories for Materials Testing and Research).

Since February 2007, the CO concentrations are measured with a custom gas chromatograph equipped with a reduction gas detector (GC-RGD), Trace Analytical RGD2. Every 15 min, an air sample is injected into the gas chromatograph for separation, and then analysed for CO concentration via mercury oxide reduction and detection of mercury vapours by UV absorption. Each analysis sample is alternated with a calibration sample by means of real air working standards with concentrations representative for ambient air concentration for the Northern Hemispheric troposphere. The working

ACPD
12, 21399–21435, 2012

standards were prepared at Max-Planck-Institute for Biogeochemistry in Jena and referenced against the CSIRO/1999 scale. This guarantees a continuous check of the detector calibration (Novelli, 1999) with accuracy higher than ±0.5 % of the recorded CO concentration values.

Continuous measurements of equivalent BC (hereafter BC) are obtained by a multi-angle absorption photometer (MAAP 5012, Thermo Electron Corporation) since March 2006. The reduction of light transmission at 670 nm, multiple reflection intensities, and air sample volume are continuously integrated over the sample run period to provide a real time data output (1 min resolution, variable integration time) of BC concentration (Petzold et al., 2002).

To neglect the variability related with annual to seasonal scales, not captured by FLEXPART, we calculated tracer anomalies (ΔO_3, ΔCO, ΔBC) by subtracting a 21-day running means from the 3-h averaged values. These anomalies were used for the combined analyses with FLEXPART outputs. During the period January 2007–June 2009, for which FLEXPART outputs are available (with only a data gap in July 2008), data coverage of 76 %, 97 % and 72 % have been achieved for CO, O_3 and BC, respectively.

2.2 FLEXPART simulations

The Lagrangian particle dispersion model FLEXPART (Stohl et al., 2005) was used to quantify the impact of anthropogenic and BB emissions on the observed CO, BC and O_3 variability at ICO-OV. To this aim, 20 days backward (so-called "retroplume") simulations were done for ICO-OV location with a time resolution of 3 h (http://transport.nilu.no/projects/eucaari).

Every simulation consists of 40 000 particles released in the volume of air sampled. The backward simulations are done with full turbulence and convection parameterizations. The FLEXPART retroplume model output is proportional to the residence time of the particles in a given volume of air and corresponds to a potential emission sensitivity. When convolved with the gridded CO emission fluxes from an emission inventory, maps

ACPD
12, 21399–21435, 2012

of potential source contributions are obtained. Integrating these maps over the globe or over certain regions of specific interest (e.g. Europe, North America), yields a model-calculated CO tracer mixing ratio at the ICO-OV location. Since FLEXPART does not account for CO emissions older than 20 days, this model-calculated CO can only explain a fraction of the CO mixing ratio observed at the ICO-OV, thus providing useful hints about specific contributions still not mixed within the tropospheric background. FLEXPART considers both BB (hereinafter CO_{fire}) and anthropogenic CO emissions (hereinafter CO_{ant}). CO_{fire} emissions are estimated from fire observations obtained from MODIS on board the Aqua and Terra NASA satellites (Justice et al., 2002; Giglio et al., 2003). Hot spots detected with a confidence of 75 % or greater are used and combined with a land inventory with 1-km resolution to provide an emissions inventory. It is assumed that area burned is 180 ha per fire detection. A parameterization was applied to determine the biomass available to burning, the fraction actually burned, and the emission factors, which are all dependent on land use (see Stohl et al., 2007, for a description). For CO_{ant}, EDGAR version 3.2 emission inventory for the year 2000 (fast track) on a $1 \times 1^{\circ}$ grid was used outside North America and Europe. Over Europe, the EMEP emission inventory for the year 2005 with a resolution of 0.5 degree was used. Over most of North America, the inventory of Frost and McKeen (2006) was used.

For the purpose of systematically evaluating the influence at ICO-OV of BB and anthropogenic emissions with age less than 20 days and thus still not mixed within the atmospheric background, we analysed the time series of CO_{fire} and CO_{ant} emitted over the global domain.

FLEXPART also provides the information on the time spectrum of emission. In order to have a synthetic diagnostic, we defined a "dominant" emission age for BB and anthropogenic emissions as the time (prior to observation and expressed in days) when the total CO_{fire} and CO_{ant} contributions reached 75 % of their 20-day integrated concentration. Alternatively, emission age was also estimated by identifying the time when CO presented the maximum increase along the backward Lagrangian simulation. However, since no substantial differences were observed, only the first method is used in

ACPD
12, 21399–21435, 2012

this paper. O_3, CO and BC ICO-OV observations are averaged over 3-h to compare directly to FLEXPART data.

3 Results

3.1 Atmospheric tracer annual cycles at ICO-OV

3.1.1 Carbon monoxide (CO)

Figure 1 reports the annual cycle of CO. During 2007–2009, the average CO concentration at ICO-OV was 122 ± 7 ppbv (in terms of mean ± expanded uncertainty) at a confidence level of 95 %. The annual CO cycles were characterised by the highest monthly values from February to April and minima from June to September (only months with data coverage larger than 15 days have been reported). Increasing CO concentrations are observed during autumn. Not-negligible inter-annual variability characterised CO levels at ICO-OV. In particular, high CO concentrations were observed during spring and autumn 2007 with mixing ratios exceeding by 20 ppbv the average values during 2008–2009. Both in term of annual shape and temporal variability, the CO seasonal cycles at ICO-OV are well comparable with thoseat other high-altitude mountain sites in Europe (Zelwegger et al., 2009; Gilge et al., 2010). The observed annual cycle results from varying contributions by natural and anthropogenic emissions, production vs. removal processes and atmospheric transport (e.g. Yurganov et al., 1999; Chevalier et al., 2008; Gilge et al., 2010). In particular, the slower chemical destruction leads to a longer CO lifetime in winter and subsequent accumulation, thus explaining the observed late winter/early spring peak. Long-range transport can play a significant role in determining the seasonal cycle: in fact, as pointed out by Pfister et al. (2004), Asian and North American anthropogenic CO sources can significantly impact tropospheric Europe between January and March in addition to continental emissions. Another possible contribution that will be explored later comes from BB emissions that strongly

ACPD
12, 21399–21435, 2012

impact CO variability during specific episodes (e.g. Yurganov et al., 2005; Cristofanelli et al., 2009; Zellweger et al., 2009).

3.1.2 Surface ozone (O_3)

The observed average O_3 concentration for the years 2007–2009 at ICO-OV was 54 ± 3 ppbv, in good agreement with earlier measurements (Cristofanelli et al., 2006). The annual O_3 cycle is characterised by a winter minimum and two peaks: (1) in spring (in April, for the three years here considered) and (2) in summer (from July to August). This is a common feature for high-altitude measurement sites in Europe (e.g. Chevalier et al., 2007; Gilge et al., 2010). The summer peak is usually explained by increased photochemical production of O_3 in the lower troposphere: summer fair and warm weather conditions contribute to direct O_3 production from anthropogenic precursors and favour the export of polluted air masses from the boundary layer to the free troposphere of continental Europe (Henne et al., 2005; Cristofanelli et al., 2007). At middle latitudes in the Northern Hemisphere, the spring O_3 maximum can be related to the accumulation of precursors (as seen at ICO-OV for CO) during winter and subsequent O_3 production (Monks, 2000; Virganzan, 2004). Stratosphere-to-troposphere transport (STT) might also increase O_3 concentrations at ICO-OV during spring (Stohl et al., 2000), even if more recent analyses (Cristofanelli et al., 2006) also indicate high STT influence during autumn and winter.

3.1.3 Equivalent black carbon (BC)

The average monthly BC concentration during the year 2007–2009 was $213 \pm 34\,\mathrm{ng\,m^{-3}}$. This value is comparable with typical average levels recorded at European continental background sites (Van Dingenen et al., 2004; Putaud et al., 2004b). Similarly to O_3, the annual cycle is characterised by the presence of a winter minimum (December–January) and maxima in spring (April–May) and late summer (August–September). This behaviour probably reflects the higher efficiency of uplift during

ACPD
12, 21399–21435, 2012

warmer months and the subsequent transport of polluted air masses from the boundary layer to the measurement site (Marinoni et al., 2008; Cristofanelli et al., 2007). Interestingly, a secondary minimum in BC was observed during June when wet deposition is expected to peak, due to maximum rainfall. Large variability characterises the BC annual cycle with monthly values spanning almost an order of magnitude from 50 ng m^{-3} to 400 ng m^{-3}.

4 Role of biomass burning

The identification of BB events at ICO-OV is done here based on a combination of observation and model analysis.

The first step is to quantify the monthly mean contribution of CO_{fire} at ICO-OV to provide an estimate of the mean impact and its seasonal variability. Figure 2 shows that FLEXPART CO_{fire} was low for most part of the investigation period with an annual average value of 2.5 ppbv. It contributed only up to 2.6 % to the mean CO observed at ICO-OV during 2007–2009. Only few events (about 3 % of the entire data-set) were characterised by CO_{fire} exceeding 10 ppbv and the highest CO_{fire} values (up to 200 ppbv) were observed at the end of August 2007 when a strong BB plume was detected at ICO-OV (see Cristofanelli et al., 2009). The CO_{fire} contribution shows a clear annual cycle with the highest values during the warm months: maximum monthly average values were observed in July/September (4.2 and 3.6 ppb, respectively) and August (8.6 ppb) and a secondary maximum in late spring (4.0 ppbv in May). As deduced by the increase in the lowest percentiles of the monthly distributions (Fig. 2), these higher values were due both to an increase of the CO_{fire} baseline value and to the occurrence of specific events, as testified by the large upper percentiles.

Figure 3 reports CO concentrations observed at ICO-OV (black points) together with calculated FLEXPART CO_{fire} (red line). Data for which simultaneous FLEXPART CO_{fire} continuously exceeded 10 ppbv for more than 12 h are highlighted with coloured dots, scaled on the fire emission age. Following FLEXPART, CO_{fire} enhancements occur

ACPD
12, 21399–21435, 2012

sporadically and for a limited period of time, with 16 events with a duration ranging from 12 to 72 h: BB transport at ICO-OV accounted for a total of 21 days over the three years. Basing on the FLEXPART analyses, for these events the transport of BB emissions occurs at very different scales: six events originated from the SE/MB region, two events from the Balkan peninsula, one event from Russia. Long range transport may have a likely role with 5 events from North America, one from Central America and one from equatorial Africa. The majority of BB events (11) occurred from May to September, thus confirming that transport of BB emissions mostly occurred during warm months.

We identify five main events (24–25 April 2007, 28 August–1 September 2007; 23–24 March 2009; 28 March–1 April 2009, 1–4 May 2009), during which FLEXPART CO_{fire} increases were observed simultaneously with significant CO variations at ICO-OV. According to FLEXPART, these events are due to: (i) local transport of BB emissions from Central Alps (event I) and North Africa, South Italy and Greece (event II), (ii) regional transport from Russia (event V), (iii) global scale transport from North America (event III) and West Equatorial Africa (event IV). Supplementary materials presents the CO_{fire} source contribution maps for each of these events (Figs. S1–S5), while Table 1 reports the CO, O_3 and BC concentrations: CO_{fire} contributions ranged from 10.1 % to 47.5 % of the observed CO mixing ratio. Events I, II and V are characterized by clear CO enhancements ($\Delta CO > 0$ ppb) in respect to the average behaviour obtained by applying the 21-day running mean. Events III and IV, related with long range transport of BB emissions, were instead characterised by CO decreases ($\Delta CO < 0$ ppb). The actual concentration of CO due to a more aged and distant BB may be highly variable due to a combination of processes that is difficult to evaluate and that may lead to the negative observed CO anomaly. As an example, Real et al. (2007) showed that the mixing ratio of CO in forest fire plumes decreases by 50 % during a 5-day transport due to atmospheric mixing. Moreover, for the event IV, injection of BB emissions into tropical air masses with low pre-existing CO concentrations may lead to CO values still lower than those typically observed in the middle latitudes (WMO, 2011). Thus, the advection

ACPD
12, 21399–21435, 2012

of this plume can lead to a decrease of observed CO at ICO-OV, even in the presence of a substantial BB contribution. This could explain the significant negative correlation existing between the FLEXPART CO_{fire} and the CO mixing ratio observed at ICO-OV during the episode IV (see Table 1).

O_3 has a large variability among the identified fire plumes, with mean mixing ratios ranging from 45.2 ppbv to 88.5 ppb: overall, 4/5 events show O_3 enhancement from the 21-day filtered time series ($\Delta O_3 > 0$ ppb). Figure 4a shows the relationship between CO and O_3 mixing ratios observed at ICO-OV during the five events. In order to remove the correlation due to the diurnal cycle of CO and O_3 at ICO-OV (see e.g. Cristofanelli et al., 2009), here we considered the residuals of 3-h averaged concentration (CO^{res}, O_3^{res}, BC^{res}) with respect to the mean diurnal variation estimated in the 21 days around the BB event. The different scatter of data among the detected events (with R values ranging from −0.14 for the event III to 0.93 for the event I) is indicative of a great variability of chemical reactivity in air-masses potentially impacted by BB.

Previous studies (see Val Martin et al., 2006 and references therein) showed that the slope of the linear fit of O_3 versus CO can be used to evaluate the O_3/CO enhancement ratio (ER), i.e. the amount of O_3 molecule produced per CO molecule emitted. We calculated the linear fit by applying the reduced major axis (RMA) technique to four events characterised by O_3-CO linear correlation coefficients larger than 0.30 (see Table 1). The range of the positive O_3/CO ER (0.27–0.71) was in relatively good agreement with previous characterization of BB plumes. Val Martin et al. (2006) reported ER ranging from 0.14 to 0.89 in boreal fire plumes observed at the Azores Islands, while Bertschi and Jaffe (2005) found ER from 0.15 to 0.84 in plumes from Asian boreal wildfires over Northwest US, suggesting that significant O_3 production can occur in BB plumes probably due to the slow recycling of PAN, HNO_3 and organic nitrates (Honrath et al., 2004; Bertschi and Jaffe, 2005). A negative value of −0.22 is observed during event IV. Negative or not-significant O_3/CO ER have been already observed in aged BB plumes by Val Martin et al. (2006) and Real et al. (2007). This was attributed to the high aerosol concentrations within fire emission plumes or other processes affect-

ACPD
12, 21399–21435, 2012

ing nighttime chemistry (i.e. hydrolysis of N_2O_5) as well as O_3 loss by reaction with organic compounds during long-range transport. Real et al. (2006) showed that the strong aerosol light extinction in dense BB smoke plumes can decrease O_3 formation efficiency. In our case, a strong Saharan dust transport event was also detected at ICO-OV by in-situ and satellite (MODIS) observations. This could possible lead to heterogeneous removal of O_3 and its precursors (via HNO_3 and NO_3 depletion) and by decreasing photolysis rate (e.g. He and Carmichel, 1999; Balis et al., 2000; Harrison et al., 2001). Depletion of ozone in Saharan dust layers was systematically observed at ICO-OV by Bonasoni et al. (2004).

BC concentrations are highly variable during the events, ranging from 44.1 $ng\,m^{-3}$ to 1072.3 $ng\,m^{-3}$ (Table 1). BC concentrations showed positive anomalies with respect to the 21 days average for events I, II, III and V and negative for event IV which was characterised by the lowest BC concentrations indicating that removal processes may have been important. BC^{res} as a function of CO^{res} is reported in Fig. 4b and all the analysed events show significant positive correlation; the linear correlation coefficient R ranges from 0.31 (event IV) to 0.94 (event II). The BC^{res}/CO^{res} slopes were very similar, except for event IV. RMA analysis gives BC/CO ERs value ranging from 2.69 to 29.83 (Table 1). Previous observations of BB (from North America and Siberia) at baseline stations in the Azores (Val Martin et al., 2006), Ireland (Forster at al., 2001) an Japan (Kaneyasu et al., 2007) reported BC/CO ERs ranging from 0.5 to 8.4. Warneke et al. (2009) and Kondo et al. (2011) reported ERs of 8.5 ± 5.4 and $10 \pm 5\,ng\,m^{-3}$/ppbv for BB in Asia (Sibera and Kazakhstan). Pan et al. (2011), reported BC/CO ratio of 10.3 ± 0.3 and $11.6 \pm 0.5\,ng\,m^{-3}\,ppbv^{-1}$ for BB plumes observed at the background station Mt. Huang (1840 m a.s.l.) in East China. Thus, while events I, II and IV showed ERs in good agreement with already published values, events III and V were characterised by significant higher values. It is not entirely clear why the BC-CO slopes were so large, but different explanations could be considered, especially for event V. Firstly, these high BC/CO ERs may be explained by high combustion efficiency of the source fires (e.g. Kondo et al., 2011). Secondly, Pan et al. (2011) showed that BC/CO ERs are strongly influ-

ACPD
12, 21399–21435, 2012

enced by rain washout and/or large environmental RH along the transport pathways. In particular, dry conditions dominated at ICO-OV during event V, with RH values well below 60 %. Moreover, as deduced by the analysis of meteorological analyses based on GDAS-NCEP data set, also along the transport path, dry conditions prevailed for this event (average RH values: 59 %), suggesting that rain washout or removal processes in high RH environment were unlikely for this specific event. Finally, it cannot be completely excluded anthropogenic contribution within BB plumes, which can increase the slope of the BC-CO correlation. As reported by Cristofanelli et al. (2009), at ICO-OV, anthropogenic pollution plumes from the polluted Po basin can be characterised by ERs higher than 14 ng m^{-3} ppbv^{-1}. FLEXPART retroplume analyses (here not shown) indicated significant footprint emission sensitivity over the Central/Northern France and the Eastern Po basin for the air-masses reaching ICO-OV during event III and V, respectively. Thus, it is possible that mixing with polluted air-masses occurred 1–2 days before the arriving of air-masses at the measurement site.

5 Role of anthropogenic emissions

We turn now on the role of anthropogenic emissions in affecting atmospheric composition at ICO-OV based on the observations of ΔO_3, ΔCO, and BC and on the CO_{ant} calculated by FLEXPART. The 20-day old FLEXPART CO_{ant} concentrations have an average value of 22.4 ppbv, which corresponds to 17.4 % of the mean CO value observed at ICO-OV during the same period. It is difficult to recognise a clear yearly cycle of CO_{ant} (Fig. 5): the highest monthly concentration of CO_{ant} is found for April (27.7 ppb) and the lowest ones in autumn and early winter (January 16.8 ppbv, October 19.3 ppbv and November 18.5 ppbv). In particular, April 2007 was characterised by higher average CO_{ant} (+25 %) than April 2008 and 2009, in good agreement with the highest observed CO concentrations at ICO-OV (see Fig. 1). This suggests that, the transport variability of anthropogenic CO simulated by FLEXPART, can explain part of the interannual CO variability observed at ICO-OV.

ACPD
12, 21399–21435, 2012

Larger upper percentiles of FLEXPART CO_{ant} indicate that spring and summer (from April to September) are more affected by episodes with air-masses rich in anthropogenic CO. These events are typically due to relatively fresh emissions. The emission age median value for April–September is only 72 h, whereas it is 114 h from October to February. This can be explained by the more efficient export of CO from the planetary boundary layer to the altitude of ICO-OV during summer. FLEXPART also gives high CO_{ant} concentrations in December with upper quantiles similar to those seen for the warm months. However, the median emission age (129 h) is much higher than in summer. Even if a significant fraction of these high CO_{ant} were still related with moderately aged (less than 96 h) European emissions, transport from North America significantly increased the emission age at ICO-OV during specific periods (e.g. 3–11 December 2008). This is in agreement with previous work showing that inter-continental transport can be a relevant source of polluted air-masses over Europe (e.g. Stohl and Trickl, 1999; Trickl et al., 2003).

Figure 6 reports the observed anomalies of CO, O_3 for three seasons corresponding to the yearly observed CO maximum (January–April), minimum (May–September) and transition period (October–December) for the 30-month investigation period. ΔCO and ΔO_3 have been reported as a function of observed BC concentrations and CO_{ant} emission age (coloured scales). In order to reduce the effect of diurnal variations caused by thermal circulations and local photochemistry, data have been averaged over a 12 h period centred around 00:00 and 12:00 UTC + 1. Correlation between ΔCO and ΔO_3 is strong and positive in May–September (R: 0.79), indicating photochemical O_3 formation. In particular, enhanced ΔCO and ΔO_3 are observed with the presence of high BC concentration ($> 400\,ng\,m^{-3}$). This indicates that polluted air-masses influenced by combustion emissions significantly contributed to the presence of the highest O_3 and CO values observed at ICO-OV during late spring and summer. On the other hand, ΔO_3 is not correlated with ΔCO during January–April (R: −0.07). Nevertheless, the highest BC values ($> 400\,ng\,m^{-3}$) were still observed together with positive ΔCO and ΔO_3. During October–December, ΔCO and ΔO_3 were negatively correlated (R: −0.51)

ACPD
12, 21399–21435, 2012

indicating reduced photochemical production and/or O_3 depletion due to NO titration. In particular, positive ΔO_3 mostly coincides with negative ΔCO and low BC values, indicating that clean air-masses, possibly from the free troposphere or the lower stratosphere (e.g. Cristofanelli et al., 2006) could lead to O_3 increase during these months.

Figure 6 also shows that, for May–September, the greatest fraction of observations tagged to $CO_{ant} < 7$ days were mostly associated with enhanced ΔCO, ΔO_3 and BC. However, positive CO and O_3 anomalies with enhanced BC values were also present with older CO_{ant} emission age (up to 15 days), indicating that anthropogenic emissions occurring at very different temporal scales affected tracer concentrations at ICO-OV. In January–April, it is less straightforward to identify clear signatures of CO_{ant} emission age with observed atmospheric composition, even if positive ΔCO still occur with younger CO_{ant} emission ages. However, the highest BC concentrations ($400\,ng\,m^{-3}$) were mostly associated with emission ages ranging from 7 to 11 days, thus suggesting a contribution by slower or farther polluted air-mass transport. From October to December, FLEXPART calculations do not show the presence of significant recent emissions (i.e. less than 5 days), indicating again that during these months ICO-OV is mostly influenced by emissions with longer times of atmospheric transport.

In order to quantify the amount of observed variability that can be ascribed to transport diagnosed by FLEXPART, Fig. 7 reports the seasonal correlation between ΔCO, ΔO_3 and BC with CO_{ant} for 24-h time average. The days influenced by the BB transport events identified in the previous Section were not treated in this analysis. Correlation between FLEXPART CO_{ant} with observed ΔCO increases with the length of the time averaging window between 3 and 24 h because the effect of short timing errors in modelled contributions is reduced by increasing the average time window. Correlations decrease for even longer averaging times, so we present the results obtained for the 24 h analysis. FLEXPART CO_{ant} correctly reproduce the absolute range of ΔCO variability observed at ICO-OV (−30/30 ppbv): in fact, as reported by Fig. 7, CO_{ant} ranged from 0 to 60 ppbv. The slope of the linear correlation between ΔCO and CO_{ant} varies from 0.24 (January–April) to 0.70 (May–September). The calculated ΔCO-CO_{ant} linear cor-

ACPD
12, 21399–21435, 2012

relation coefficients (R) are statistically significant at the 95 % confidence level for all the seasonal aggregations. This suggests that an important fraction of the observed CO variability can be explained by anthropogenic emissions, especially in May–September when the strongest linear coefficient has been found (R = 0.61).

Maximum CO_{ant}-O_3 correlation is also obtained in May–September, indicating the important role of anthropogenic emissions for O_3 formation during the warm months. As for ΔCO, the highest positive ΔO_3 were tagged to emissions younger than 5–7 days even if contribution from older emissions cannot be neglected, indicating that anthropogenic emissions transported on very different scales affected tracer concentrations at ICO-OV. In agreement with the results shown in Fig. 6, for ΔO_3 the linear correlation is negative (and significant at the 95 % confidence level) during October–December and the few observations tagged to young anthropogenic emissions (blue dots) were generally characterised by negative ΔO_3 further stressing the possible role played by NO titration in the local-regional European PBL during these months.

For BC, the linear correlation with CO_{ant} is highest in January–April (R: 0.57): as suggested by FLEXPART it is likely that enhancement in aerosol concentrations is due to relatively aged anthropogenic emissions. Significant correlation can be seen also in May–September with BC enhancements above 400 ng m^{-3} mainly related to emission ages lower than 7 days. In October–December BC and CO_{ant} appear to be almost uncorrelated with BC concentrations never increased up to 300 ng m^{-3} and minimum values of CO_{ant} (see Fig. 5).

6 Summary

We quantified the variability of O_3, CO and BC at the Mt. Cimone global GAW-WMO station (ICO-OV) and we investigated the influence of biomass burning (BB) and anthropogenic emissions younger than 20 days.

In 2007–2009, the average O_3, CO and BC concentrations at ICO-OV were 54 ± 3 ppbv, 122 ± 7 ppbv and 213 ± 34 ng m^{-3} (mean ± expanded uncertainty with p <

ACPD
12, 21399–21435, 2012

95 %), with marked seasonal cycles characterized by summer maxima–winter minima for O_3 and BC, and a spring maximum–summer minimum for CO.

According to the FLEXPART simulations, impact of 20-day old BB emissions is maximized during the warm months from May to September when CO emitted by the identified fires specifically contributed to 4 % of the CO observed at the ICO-OV, with a maximum of 12 % in August. BB emissions traced back by FLEXPART had a significant impact on the observed tracers only during specific events when CO emitted by BB contributed from 10 % up to 45 % to the observed CO mixing ratio: as diagnosed by FLEXPART, BB plumes at ICO-OV occurred for 21 days over the 30 months here considered. It should be clear in mind that these values represent minimal estimates about BB influence, since FLEXPART cannot quantify the contributions coming from the well-mixed background.

Five major BB transport events have been evaluated in detail relating observed local variations of O_3, CO and BC to transport scales (global, regional and local), source regions and enhancement ratios (ERs). Very large variability of enhancement ratios for O_3/CO (from 0.26 to 0.71 ppb/ppb) and for BC/CO (from 2.69 to 29.83 $ng\,m^{-3}$/ppb) were observed at ICO-OV during these events. The O_3/CO ERs appeared to be in fair agreement with the values found in previous studies (Bertische and Jaffe, 2005; Val Martin et al., 2006) but for some events the BC/CO ERs were higher than values reported in literature which ranged up to $\sim$ 10–12 $ng\,m^{-3}\,ppbv^{-1}$ (e.g. Val Martin et al., 2006; Forster at al., 2001; Kaneyasu et al., 2007).

On a quantitative basis, observed CO anomalies correlated significantly with FLEXPART 20-day old anthropogenic CO contributions (CO_{ant}) with similar ranges of variability: −30 to +30 ppbv for CO and 0–60 ppbv for CO_{ant}. As indicated by FLEXPART, CO_{ant}, can explain 17.4 % of the mean CO value observed at ICO-OV during the investigating period, with the warm months (from April to September) appearing to be particularly affected by transport events of air-masses rich in anthropogenic CO. Overall, the average age of the FLEXPART CO tracer is just 3 days, showing that the CO sources occurred from local to regional scales. Also during winter (especially on De-

ACPD
12, 21399–21435, 2012

cember) moderately aged (4 days) anthropogenic emissions affected the measurement site frequently, suggesting advection of polluted air-masses from continental Europe. However, specific transport episodes of polluted air-masses from the North America PBL could also affect ICO-OV, as occurred between 3 and 11 December 2008, when CO significantly increased at ICO-OV (+11 ppb) and CO_{ant} from North America almost doubled the CO_{ant} from Europe.

The analysis of the seasonal correlation among CO, O_3 and BC observed at the ICO-OV as a function of the CO_{ant} emission age, allowed to identify three main regimes. During May–September, significant positive correlation (R: 0.79) has been found for CO and O_3. The highest CO and O_3 values were observed in presence of high BC concentration ($> 400\,ng\,m^{-3}$), indicating significant photochemical O_3 formation in air-masses influenced by anthropogenic combustion emissions occurring from regional to global scales. On the other side, CO and O_3 were negatively correlated (R: −0.51) during October–December, when FLEXPART does not show significant presence of recent anthropogenic emissions and only a few observations are characterized by enhanced BC. Such behaviour may be attributed to an ensemble of processes concurrent in enhancing O_3 with low CO (i.e upper troposphere/lower stratosphere intrusions) and O_3 titration with NO in polluted air-masses along with low photochemical activity. An intermediate situation occurs in January–April with CO and O_3 almost uncorrelated and BC enhancements mainly associated to relatively old (> 7 days) anthropogenic emissions. Overall, the correlation analysis of ICO-OV tracers with CO_{ant} indicated that the fraction of observed variability ascribed to 20-day old anthropogenic emissions ranged from 22 % (in January–April) to 37 % (in May–September) for ΔCO, from 1 % (in October–December) to 19 % (in May-September) for ΔO_3 and from less than 1 % (in October–December) to 32 % (in January–April) for BC.

This work lead to the conclusion that trace gas and BC concentrations at the ICO-OV, which can be considered representative for SE/MB, are partially driven by local to global scale transport of anthropogenic emissions while, as diagnosed by FLEXPART, BB appeared to have a minor impact on the annual mean. Further work is needed to

ACPD
12, 21399–21435, 2012

explore the validity of the results here obtained for other sites in the SE/MB region, that can be affected by different transport patterns and/or emissions.

Supplementary material related to this article is available online at: http://www.atmos-chem-phys-discuss.net/12/21399/2012/acpd-12-21399-2012-supplement.pdf.

Acknowledgements. This research has been supported by the SHARE (Stations at High Altitudes for Environmental Research) Project thanks to contributions from the Italian National Research Council and the Italian Ministry of Foreign Affairs and by ACTRIS, funded within the EC 7th Framework Programme under "Research Infrastructures for Atmospheric Research".

References

Andreae, M. O. and Gelencsér, A.: Black carbon or brown carbon? The nature of light-absorbing carbonaceous aerosols, Atmos. Chem. Phys., 6, 3131–3148, doi:10.5194/acp-6-3131-2006, 2006.

Auvray, M., Bay, I.: Long-range transport to Europe: seasonal variations and implications for the European ozone budget, J. Geophys. Res., 110, D11303, doi:10.1029/2004JD005503, 2005.

Balis, D., Papayannis, A., Galani, E., Marenco, F., Santacesaria, V., Hamonou, E., Chazette, P., Ziomas, I., Zerefos, C.: Tropospheric LIDAR aerosol measurements and sun photometric observations at Thessaliniki, Greece, Atmos. Environ., 34, 925–932, 2000.

Bertschi, I. T. and Jaffe, D. A.: Long-range transport of ozone, carbon monoxide, and aerosols to the NE Pacific troposphere during the summer of 2003: observations of smoke plumes from Asian boreal fires, J. Geophys. Res., 110, D05303, doi:10.1029/2004JD005135, 2005

Bonasoni, P., Stohl, A., Cristofanelli, P., Calzolari, F., Colombo, T., and Evangelisti, F.: Background ozone variations at Mt. Cimone Station, Atmos. Environ., 34, 5183–5189, 2000.

Bonasoni, P., Cristofanelli, P., Calzolari, F., Bonafè, U., Evangelisti, F., Stohl, A., Zauli Sajani, S., van Dingenen, R., Colombo, T., and Balkanski, Y.: Aerosol-ozone correlations during

ACPD

12, 21399–21435, 2012

dust transport episodes, Atmos. Chem. Phys., 4, 1201–1215, doi:10.5194/acp-4-1201-2004, 2004.
Bond, T. C., Streets, D. G., Yarber, K. F., et al.: A technology based global inventory of black carbon and organic carbon emissions from combustion, J. Geophys. Res., 109, D14203, doi:10.1029/2003JD003697, 2004.
Bond, T. C., Zarzycki, C., Flanner, M. G., and Koch, D. M.: Quantifying immediate radiative forcing by black carbon and organic matter with the Specific Forcing Pulse, Atmos. Chem. Phys., 11, 1505–1525, doi:10.5194/acp-11-1505-2011, 2011.
Conti, S., Meli, P., Minelli, G., Solimini, R., Toccaceli, V., Vichi, M., Beltrano, C., and Perini, L.: Epidemiologic study of mortality during the summer 2003 heat wave in Italy, Environ. Res., 98, 390–399, 2005.
Chevalier, A., Gheusi, F., Delmas, R., Ordóñez, C., Sarrat, C., Zbinden, R., Thouret, V., Athier, G., and Cousin, J.-M.: Influence of altitude on ozone levels and variability in the lower troposphere: a ground-based study for western Europe over the period 2001–2004, Atmos. Chem. Phys., 7, 4311–4326, doi:10.5194/acp-7-4311-2007, 2007.
Chevalier, A., Gheusi, F., Attié, J.-L., Delmas, R., Zbinden, R., Athier, G., and Cousin, J.-M.: Carbon monoxide observations from ground stations in France and Europe and long trends in the free troposphere, Atmos. Chem. Phys. Discuss., 8, 3313–3356, doi:10.5194/acpd-8-3313-2008, 2008.
Cristofanelli, P., Bonasoni, P., Tositti, L., Bonafè, U., Calzolari, F., Evangelisti, F., Sandrini, S., and Stohl, A.: A 6-yr analysis of stratospheric intrusions and their influence on ozone at Mt. Cimone (2165 m a.s.l.), J. Geophys. Res., 111, D03306, doi:10.1029/2005JD006553, 2006.
Cristofanelli, P., Bonasoni, P., Carboni, G., Calzolari, F., Casarola, L., Zauli Sajani, S., and Santaguida, R.: Anomalous high ozone concentrations recorded at a high mountain station in Italy in summer 2003, Atmos. Environ., 41, 1383–1394, 2007.
Cristofanelli, P., Marinoni, A., Arduini, J., Bonafè, U., Calzolari, F., Colombo, T., Decesari, S., Duchi, R., Facchini, M. C., Fierli, F., Finessi, E., Maione, M., Chiari, M., Calzolai, G., Messina, P., Orlandi, E., Roccato, F., and Bonasoni, P.: Significant variations of trace gas composition and aerosol properties at Mt. Cimone during air mass transport from North Africa – contributions from wildfire emissions and mineral dust, Atmos. Chem. Phys., 9, 4603–4619, doi:10.5194/acp-9-4603-2009, 2009.
Crutzen, P. J. and Andreae, M. O.: Biomass burning in the tropics: impact on atmospheric chemistry and biogeochemical cycles, Science, 250, 1669–1678, 1990.

ACPD
12, 21399–21435, 2012

Crutzen, P. J., Lawrence, M. G., and Pöschl, U.: On the background photochemistry of tropospheric ozone, Tellus, 51, 123–146, 1999.

Duncan, B. N., West, J. J., Yoshida, Y., Fiore, A. M., and Ziemke, J. R.: The influence of European pollution on ozone in the Near East and Northern Africa, Atmos. Chem. Phys., 8, 2267–2283, doi:10.5194/acp-8-2267-2008, 2008.

Flanner, M. G., Zender, C. S., Hess, P. G., Mahowald, N. M., Painter, T. H., Ramanathan, V., and Rasch, P. J.: Springtime warming and reduced snow cover from carbonaceous particles, Atmos. Chem. Phys., 9, 2481–2497, doi:10.5194/acp-9-2481-2009, 2009.

Forster, C., Wandinger, U., Wotawa, G., James, P., Mattis, I., Althausen, D., Simmonds, P., O'Doherty, S., Kleefeld, C., Jennings, S. G., Schneider, J., Trickl, T., Kreipl, S., Jäger, H., and Stohl, A.: Transport of boreal forest fire emissions from Canada to Europe, J. Geophys. Res., 106, 22887–22906, 2001.

Forster, P., Ramaswamy, V., Artaxo, P., Berntsen, T., Betts, R., Fahey, D. W., Haywood, J., Lean, J., Lowe, D. C., Myhre, G., Nganga, J., Prinn, R., Raga, G., Schulz M., and Van Dorland, R.: Changes in atmospheric constituents and in radiative forcing, in: Climate Change 2007: The Physical Science Basis. Contribution of Working Group I to the Fourth Assessment Report of the Intergovernmental Panel on Climate Change, edited by: Solomon, S., Qin, D., Manning, M., Chen, Z., Marquis, M., Averyt, K. B., Tignor M., and Miller, H. L., Cambridge University Press, Cambridge, UK and New York, NY, USA, 2007.

Fischer, H., Kormann, R., Klüpfel, T., Gurk, Ch., Königstedt, R., Parchatka, U., Mühle, J., Rhee, T. S., Brenninkmeijer, C. A. M., Bonasoni, P., and Stohl, A.: Ozone production and trace gas correlations during the June 2000 MINATROC intensive measurement campaign at Mt. Cimone, Atmos. Chem. Phys., 3, 725–738, doi:10.5194/acp-3-725-2003, 2003.

Frost, G. J., McKeen, S. A., Trainer, M., Ryerson, T. B., Neuman, J. A., Roberts, J. M., Swanson, A., Holloway, J. S., Sueper, D. T., Fortin, T., Parrish, D. D., Fehsenfeld, F. C., Flocke, F., Peckham, S. E., Grell, G. A., Kowal, D., Cartwright, J., Auerbach, N., and Habermann, T.: Effects of changing power plant NO_x emissions on ozone in the Eastern United States: proof of concept, J. Geophys. Res., 111, D12306, doi:10.1029/2005JD006354, 2006.

Gauss, M., Myhre, G., Pitari, G., Prather, M. J., Isaksen, I. S. A., Berntsen, T. K., Brasseur, G. P., Dentener, F. J., Derwent, R. G., Hauglustaine, D. A., Horowitz, L. W., Jacob, D. J., Johnson, M., Law, K. S., Mickley, L. J., Müller, J.-F., Plantevin, P.-H., Pyle, J. A., Rogers, H. L., Stevenson, D. S., Sundet, J. K., van Weele, M., and Wild, O.: Radiative forcing in the 21st

ACPD
12, 21399–21435, 2012

century due to ozone changes in the troposphere and the lower stratosphere, J. Geophys. Res., 108, 4292, doi:10.1029/2002JD002624, 2003.
Giglio, L., Descloitres, J., Justice, C. O., and Kaufman, Y.: An enhanced contextual fire detection algorithm for MODIS, Remote Sens. Environ., 87, 273–282, 2003.
Gilge, S., Plass-Duelmer, C., Fricke, W., Kaiser, A., Ries, L., Buchmann, B., and Steinbacher, M.: Ozone, carbon monoxide and nitrogen oxides time series at four alpine GAW mountain stations in central Europe, Atmos. Chem. Phys., 10, 12295–12316, doi:10.5194/acp-10-12295-2010, 2010.
Harrison, S. P., Kohfeld, K. E., Roelandt, C., and Claquin, T.: The role of dust in climate changes today, at the Last Glacial Maximum and in the future, Earth Sci. Rev., 54, 43–80, 2001.
He, S. and Carmichael, G. R.: Sensitivity of photolysis rates and ozone production in the troposphere to aerosol properties, J. Geophys. Res., 104, 26307–26324, 1999.
Henne, S., Furger, M., Nyeki, S., Steinbacher, M., Neininger, B., de Wekker, S. F. J., Dommen, J., Spichtinger, N., Stohl, A., and Prévôt, A. S. H.: Quantification of topographic venting of boundary layer air to the free troposphere, Atmos. Chem. Phys., 4, 497–509, doi:10.5194/acp-4-497-2004, 2004.
Henne, S., Dommen, J., Neininger, B., Reimann, S., Staehelin, J., and Prèvôt, A. S. H.: Influence of mountain venting in the Alps on the ozone chemistry of the lower free troposphere and the European pollution export, J. Geophys. Res., 110, D22307, doi:10.1029/2005JD005936, 2005.
Honrath, R. E., Owen, R. C., Val Martın, M., Reid, J. S., Lapina, K., Fialho, P., Dziobak, M. P., Kleissl, J., and Westphal, D. L.: Regional and hemispheric impacts of anthropogenic and biomass burning emissions on summertime CO and O_3 in the North Atlantic lower free troposphere, J. Geophys. Res., 109, D24310, doi:10.1029/2004JD005147, 2004.
Huntrieser, H., Heland, J., Schlager, H., Forster, C., Stohl, A., Aufmhoff, H., Arnold, F., Scheel, H. E., Campana, M., Gilge, S., Eixmann, R., and Cooper, O.: Intercontinental air pollution transport from North America to Europe: experimental evidence from airborne measurements and surface observations, J. Geophys. Res., 110, D01305, doi:10.1029/2004JD005045, 2005.
Justice, C. O., Giglio, L., Korontzi, S., Owens, J., Morisette, J. T., Roy, D., Descloitres, J., Alleaume, S., Petitcolin, F., and Kaufman, Y.: The MODIS fire products, Remote Sens. Environ., 83, 244–262, 2002.

ACPD
12, 21399–21435, 2012

Kaneyasu N., Igarashi, Y., Sawa, Y., Takahashi, H., Takada, H., Kumata, H., and Holler, R.: Chemical and optical properties of 2003 Siberian forest fire smoke observed at the summit of Mt. Fuji, Japan, J. Geophys. Res., 112, D13214, doi:10.1029/2007JD008544, 2007.

Kondo, Y., Matsui, H., Moteki, N., Sahu, L., Takegawa, N., Kajino, M., Zhao, Y., Cubison, M. J., Jimenez, J. L., Vay, S., Diskin, G. S., Anderson, B., Wisthaler, A., Mikoviny, T., Fuelberg, H. E., Blake, D. R., Huey, G., Weinheimer, A. J., Knapp, D. J., and Brune, W. H.: Emissions of black carbon, organic, and inorganic aerosols from biomass burning in North America and Asia in 2008, J. Geophys. Res., 116, D08204, doi:10.1029/2010JD015152, 2011.

Lelieveld, J., Berresheim, H., Borrmann, S., Crutzen, P. J., Dentener, F. J., Fischer, H., Feichter, J., Flatau, P. J., Heland, J., Holzinger, R., Kormann, R., Lawrence, M. B., Levin, Z., Markowicz, K., Mihalopoulos, N., Minikin, A., Ramanthan, V., de Reus, M., Roelofs, G. J., Scheeren, H. A., Sciare, J., Schlager, H., Schulz, M., Siegmund, P., Steil, B., Stephanou, E. G., Stier, P., Traub, M., Warneke, C., Williams, J., and Ziereis, H.: Global air pollution crossroads over the Mediterranean, Science, 298, 794–799, 2002.

Lohmann, U., Feichter, J., Penner, J. E., and Leaitch, W. R.: Indirect effect of sulfate and carbonaceous aerosols: a mechanistic treatment, J. Geophys. Res., 105, 12193–12206, 2000.

Marinoni, A., Cristofanelli, P., Calzolari, F., Roccato, F., Bonafè, U., Bonasoni, P.: Continuous measurements of aerosol physical parameters at the Mt. Cimone GAW Station (2165 m a.s.l., Italy), Sci. Total Environ., 391, 241–251, 2008.

Millàn, M., Sanz, J., Salvador, R., and Mantilla, E.: Atmospheric dynamics and ozone cycles related to nitrogen deposition in the Western Mediterranean, Environ. Pollut., 118, 167–186, 2006.

Monks, P.: A review of the observations and origins of the spring maximum, Atmos. Environ., 34, 3545–3561, 2000.

Monks, P. S., Granier, C., Fuzzi, S., Stohl, A., Williams, M. L., Akimoto, H., Amann, M., Baklanov, A., Baltensperger, U., Bey, I., Blake, N., Blake, R. S., Carslaw, K., Cooper, O. R., Dentener, F., Fowler, D., Fragkou, E., Frost, G. J., Generoso, S., Ginoux, P., Grewe, V., Guenther, A., Hansson, H. C., Henne, S., Hjorth, J., Hofzumahaus, A., Huntrieser, H., Isaksen, I. S. A., Jenkin, M. E., Kaiser, J., Kanakidou, M., Klimont, Z., Kulmala, M., Laj, P., Lawrence, M. G., Lee, J. D., Liousse, C., Maione, M., McFiggans, G., Metzger, A., Mieville, A., Moussiopoulos, N., Orlando, J. J., O'Dowd, C. D., Palmer, P. I., Parrish, D. D., Petzold, A., Platt, U., Pöschl, U., Prévôt, A. S. H., Reeves, C. E., Reimann, S., Rudich, Y., Sellegri, K., Steinbrecher, R., Simpson, D., ten Brink, H., Theloke, J., van der Werf, G. R., Vautard, R., Vestreng, V., Vla-

ACPD
12, 21399–21435, 2012

chokostas, Ch., and von Glasow, R.: Atmospheric composition change – global and regional air quality, Atmos. Environ., 43, 5268–5350, 2009.
Novelli, P. C.: CO in the atmosphere: measurement techniques and related issues, Chemosphere Global Change Sci., 1, 115–126, 1999.
Novelli, P. C., Masarie, K. A., Lang, P. M., Hall, B. D., Myers, R. C., and Elkins, J. W.: Reanalysis of tropospheric CO trends: effects of the 1997–1998 wildfires, J. Geophys. Res., 108, 4464, doi:10.1029/2002JD003031, 2003.
Pace, G., di Sarra, A., Meloni, D., Piacentino, S., and Chamard, P.: Aerosol optical properties at Lampedusa (Central Mediterranean). 1. Influence of transport and identification of different aerosol types, Atmos. Chem. Phys., 6, 697–713, doi:10.5194/acp-6-697-2006, 2006.
Pan, X. L., Kanaya, Y., Wang, Z. F., Liu, Y., Pochanart, P., Akimoto, H., Sun, Y. L., Dong, H. B., Li, J., Irie, H., and Takigawa, M.: Correlation of black carbon aerosol and carbon monoxide in the high-altitude environment of Mt. Huang in Eastern China, Atmos. Chem. Phys., 11, 9735–9747, doi:10.5194/acp-11-9735-2011, 2011.
Petzold, A., Kramer, H., and Schönlinner, M.: Continuous measurement of atmospheric black carbon using a multi-angle absorption photometer, Environ. Sci. Pollut. R., 4, 78–82, 2002.
Pfister, G., Petron, G., Emmons, L. K., Gille, J. C., Edwards, D. P., Lamarque, J. F., Attie, J. L., Granier, C., and Novelli, P. C.: Evaluation of CO simulations and the analysis of the CO budget for Europe, J. Geophys. Res.-Atmos., 109, D19304, doi:10.1029/2004JD004691, 2004.
Putaud, J.-P., Raes, F., Van Dingenen, R., Bruggemann, E., Facchini, M. C., Decesari, S., Fuzzi, S., Gehrig, R., Huglin, C., Laj, P., Lorbeer, G., Maenhaut, W., Mihalopoulos, N., Muller, K., Querol, X., Rodriguez, S., Schneider, J., Spindler, G., Ten Brink, H., Torseth, K., and Wiedensohler, A.: A European aerosol phenomenology – 2: chemical characteristics of particulate matter at kerbside, urban, rural and background sites in Europe, Atmos. Environ., 38, 2579–2595, 2004.
Real, E., Law, K. S., Weinzierl, B., Fiebig, M., Petzold, A., Wild, O., Methven, J., Arnold, S., Stohl, A., Huntrieser, H., Roiger, A., Schlager, H., Stewart, D., Avery, M., Sachse, G., Browell, E., Ferrare, R., and Blake, D.: Processes influencing ozone levels in Alaskan forest fire plumes during long-range transport over the North Atlantic, J. Geophys. Res., 112, D10S41, doi:10.1029/2006JD007576, 2007.
Seinfeld, J. H. and Pandis, S. N.: Atmospheric chemistry and physics: from air pollution to climate change, Wiley-Interscience, New York, USA, 1326 pp., 1998.

ACPD
12, 21399–21435, 2012

Simmonds, P., Manning, A., Derwent, R., Ciais, P., Ramonet, M., Kazan, V., and Ryall, D.: A burning question: can recent growth rate anomalies in the greenhouse gases be attributed to large scale biomass burning events?, Atmos. Environ., 39, 2513–2517, doi:10.1016/j.atmosenv.2005.02.018, 2005.

Solomon, S., Qin, D., Manning, M., Alley, R. B., Berntsen, T., Bindoff, N. L., Chen, Z., Chidthaisong, A., Gregory, J. M., Hegerl, G. C., Heimann, M., Hewitson, B., Hoskins, B. J., Joos, F., Jouzel, J., Kattsov, V., Lohmann, U., Matsuno, T., Molina, M., Nicholls, N., Overpeck, J., Raga, G., Ramaswamy, V., Ren, J., Rusticucci, M., Somerville, R., Stocker, T. F., Whetton, P.,Wood R. A., and Wratt, D.: Technical summary, in: Climate Change 2007: The Physical Science Basis. Contribution of Working Group I to the Fourth Assessment Report of the Intergovernmental Panel on Climate Change, edited by: Solomon, S., Qin D., Manning M., Chen Z., Marquis, M., Averyt K. B., Tignor, M., and Miller, H. L., Cambridge University Press, Cambridge, UK and New York, NY, USA, 2007.

Stohl, A. and Trickl, T.: A textbook example of long-range transport: simultaneous observation of ozone maxima of stratospheric and North American origin in the free troposphere over Europe, J. Geophys. Res., 104, 30445–30462, 1999.

Stohl, A., Spichtinger-Rakowsky, N., Bonasoni, P., Feldmann, H., Memmesheimer, M., Scheel, H. E., Trickl, T., Huebener, S. H., Ringer, W., and Mandl, M.: The influence of stratospheric intrusions on alpine ozone concentrations, Atmos. Environ., 34, 1323–1354, 2000.

Stohl, A., Huntrieser, H., Richter, A., Beirle, S., Cooper, O. R., Eckhardt, S., Forster, C., James, P., Spichtinger, N., Wenig, M., Wagner, T., Burrows, J. P., and Platt, U.: Rapid intercontinental air pollution transport associated with a meteorological bomb, Atmos. Chem. Phys., 3, 969–985, doi:10.5194/acp-3-969-2003, 2003.

Stohl, A., Forster, C., Frank, A., Seibert, P., and Wotawa, G.: Technical note: The Lagrangian particle dispersion model FLEXPART version 6.2, Atmos. Chem. Phys., 5, 2461–2474, doi:10.5194/acp-5-2461-2005, 2005.

Stohl, A., Berg, T., Burkhart, J. F., Fjæraa, A. M., Forster, C., Herber, A., Hov, Ø., Lunder, C., McMillan, W. W., Oltmans, S., Shiobara, M., Simpson, D., Solberg, S., Stebel, K., Ström, J., Tørseth, K., Treffeisen, R., Virkkunen, K., and Yttri, K. E.: Arctic smoke – record high air pollution levels in the European Arctic due to agricultural fires in Eastern Europe in spring 2006, Atmos. Chem. Phys., 7, 511–534, doi:10.5194/acp-7-511-2007, 2007.

ACPD
12, 21399–21435, 2012

Trickl, T., Cooper, O. R., Eisele, H., James, P., Mücke, R., and Stohl, A.: Intercontinental transport and its influence on the ozone concentrations over Central Europe: three case studies, J. Geophys. Res., 108, 8530, doi:10.1029/2002JD002735, 2003.

Turquety, S., Hurtmans, D., Hadji-Lazaro, J., Coheur, P.-F., Clerbaux, C., Josset, D., and Tsamalis, C.: Tracking the emission and transport of pollution from wildfires using the IASI CO retrievals: analysis of the summer 2007 Greek fires, Atmos. Chem. Phys., 9, 4897–4913, doi:10.5194/acp-9-4897-2009, 2009.

Val Martin, M., Honrath, R. E., Owen, R. C., Pfister, G., Fialho, P., and Barata, F.: Significant enhancements of nitrogen oxides, black carbon, and ozone in the North Atlantic lower free troposphere resulting from North American boreal wildfires, J. Geophys. Res., 111, D23S60, doi:10.1029/2006JD007530, 2006.

van der Werf, G. R., Randerson, J. T., Giglio, L., Collatz, G. J., Kasibhatla, P. S., and Arellano Jr., A. F.: Interannual variability in global biomass burning emissions from 1997 to 2004, Atmos. Chem. Phys., 6, 3423–3441, doi:10.5194/acp-6-3423-2006, 2006.

Van Dingenen, R., Putaud, J.-P., Martins-Dos Santos, S., and Raes, F.: Physical aerosol properties and their relation to air mass origin at Monte Cimone (Italy) during the first MINATROC campaign, Atmos. Chem. Phys., 5, 2203–2226, doi:10.5194/acp-5-2203-2005, 2005.

Vautard, R., Honoré, C., Beekmann, M., and Rouil, L.: Simulation of ozone during the August 2003 heat wave and emission control scenarios, Atmos. Environ., 39, 2957–2967, 2005.

Vingarzan, R.: A review of surface ozone background levels and trends, Atmos. Environ., 38, 3431–3442, 2004.

Volz-Thomas, A., Beekmann, M., Derwent, D., Law, K., Lindskog, A., Prevot, A., Roemer, M., Schultz, M., Schurath, U., Solberg S., and Stohl, A.: Tropospheric ozone and its control, in: Towards Cleaner Air for Europe – Science, Tools and Applications. Part 1: Results from the EUROTRAC-2; Synthesis and Integration (S&I) Project, edited by: Builtjes, P. J.-H., Harrison, R. M., Midgley, P. M., and Tørsen, K., International Scientific Secretariat, München, Germany, 73–122, 2002.

Warneke, C., Bahreini, R., Brioude, J., Brock, C. A., de Gouw, J. A., Fahey, D. W., Froyd, K. D., Holloway, J. S., Middlebrook, A., Miller, L., Montzka, S., Murphy, D. M., Peischl, J., Ryerson, T. B., Schwarz, J. P., Spackman, J. R., and Veres, P.: Biomass burning in Siberia and Kazakhstan as an important source for haze over Alaskan Arctic in April 2008, Geophys. Res. Lett., 36, L02813, doi:10.1029/2008GL036194, 2009.

ACPD
12, 21399–21435, 2012

World Meteorological Organization (WMO): Global Atmospheric Watch measurement guide, Tech. Doc. 1073, GAW Rep. 143, Geneva, Switzerland, 2002.
World Meteorological Organization (WMO): WMO WDCGG data summary, WDCGG No. 35, Japan Meteorological Agency, Tokyo, Japan, 2011.
Yurganov, L., Grechko, E., and Dzola, A.: Zvenigorod carbon monoxide total column time series: 27 yr of measurements, Chemosphere Global Change Sci., 1, 127–136, 1999.
Yurganov, L. N., Duchatelet, P., Dzhola, A. V., Edwards, D. P., Hase, F., Kramer, I., Mahieu, E., Mellqvist, J., Notholt, J., Novelli, P. C., Rockmann, A., Scheel, H. E., Schneider, M., Schulz, A., Strandberg, A., Sussmann, R., Tanimoto, H., Velazco, V., Drummond, J. R., and Gille, J. C.: Increased Northern Hemispheric carbon monoxide burden in the troposphere in 2002 and 2003 detected from the ground and from space, Atmos. Chem. Phys., 5, 563–573, doi:10.5194/acp-5-563-2005, 2005.
Zellweger, C., Hüglin, C., Klausen, J., Steinbacher, M., Vollmer, M., and Buchmann, B.: Inter-comparison of four different carbon monoxide measurement techniques and evaluation of the long-term carbon monoxide time series of Jungfraujoch, Atmos. Chem. Phys., 9, 3491–3503, doi:10.5194/acp-9-3491-2009, 2009.

ACPD
12, 21399–21435, 2012

Table 1. List of the five major BB events at ICO-OV as deduced by FLEXPART analyses. For each event we reported: start and end dates ("Date"), transport-scale ("Scale"), the emission region ("Origin"), the range (minimum, mean and maximum values) of representative emission ages during the event ("Emission age"), the averaged fraction of FLEXPART CO fire contribution ("CO_{fire} fraction"), the linear correlation coefficient between ΔCO and CO_{fire} ("R"), the mean CO and ΔCO at ICO-OV ("Mean CO"; "Mean ΔCO"), the mean O_3 and ΔO_3 at ICO-OV ("Mean O_3"; "Mean O_3"), the mean BC and ΔBC at ICO-OV ("Mean BC"; "Mean BC"), the calculated O_3-CO and BC-CO enhancement ratios ("O_3-CO ER"; "BC/CO ER").

Event	Date	Scale	Origin	Time length (h)	Emission age Min–Avg–Max (h)	CO_{fire} fraction (%)	*R* ΔCO-CO_{fire}	Mean CO (ppb)	Mean ΔCO (ppb)	Mean O_3 (ppb)	Mean ΔO_3 (ppb)	Mean BC ($ng\,m^{-3}$)	Mean ΔBC ($ng\,m^{-3}$)	O_3-CO ER	BC-CO ER
I	24–25 Apr 2007	Local	MB/SE (Alps)	19	72–72–72	13.3	0.17	196.1	40.9	88.5	14.9	1072.3	653.4	0.27	9.83
II	28 Aug–1 Sep 2007	Local	MB/SE (North Africa)	79	48–100–144	47.5	0.38	150.5	44.9	67.7	9.1	754.3	413.4	0.26	11.50
III	23–24 Mar 2009	Global	North America	16	192–196–216	14.5	0.41	139.2	−5.0	54.5	3.1	278.4	45.4	n/d	14.99
IV	28 Mar–1 Apr 2009	Global	Equatorial Africa	82	192–239–288	23.6	−0.45	136.4	−6.9	45.2	−7.8	44.1	−223.8	−0.22	2.69
V	1–4 May 2009	Regional	Russia	91	96–126–168	17.9	0.68	151.4	19.9	66.5	5.1	569.0	276.7	0.71	29.83

ACPD
12, 21399–21435, 2012

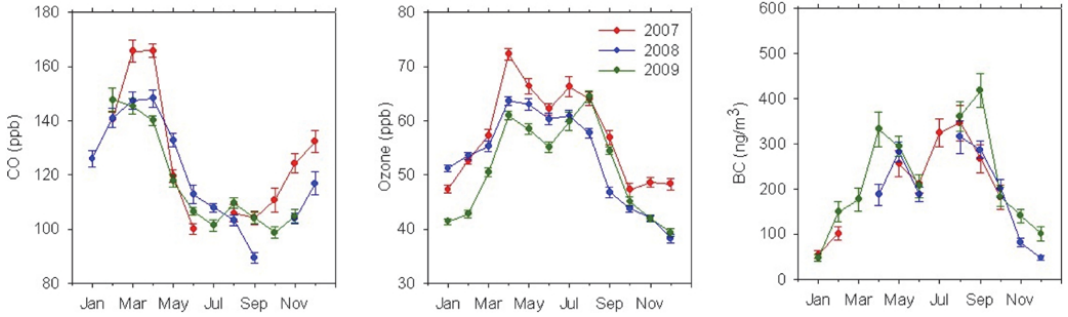

Fig. 1. Monthly means of CO, O_3 and BC at ICO-OV for the years 2007, 2008 and 2009. The error bars denote the average expanded uncertainties with $p < 95\,\%$.

ACPD
12, 21399–21435, 2012

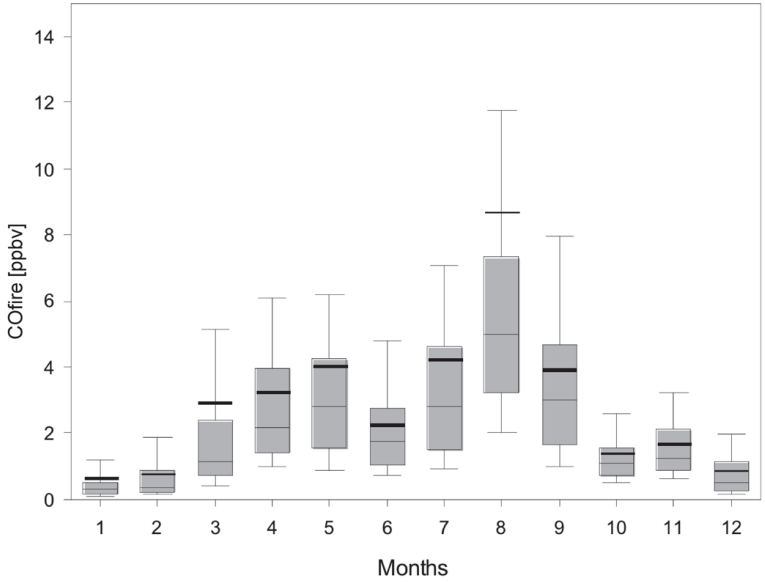

Fig. 2. Monthly distributions of FLEXPART CO_{fire} at ICO-OV during the period January 2007–July 2009. The boxes and whisker denote the 10, 25, 50, 75 and 90 percentiles. Bold lines represent average values.

ACPD
12, 21399–21435, 2012

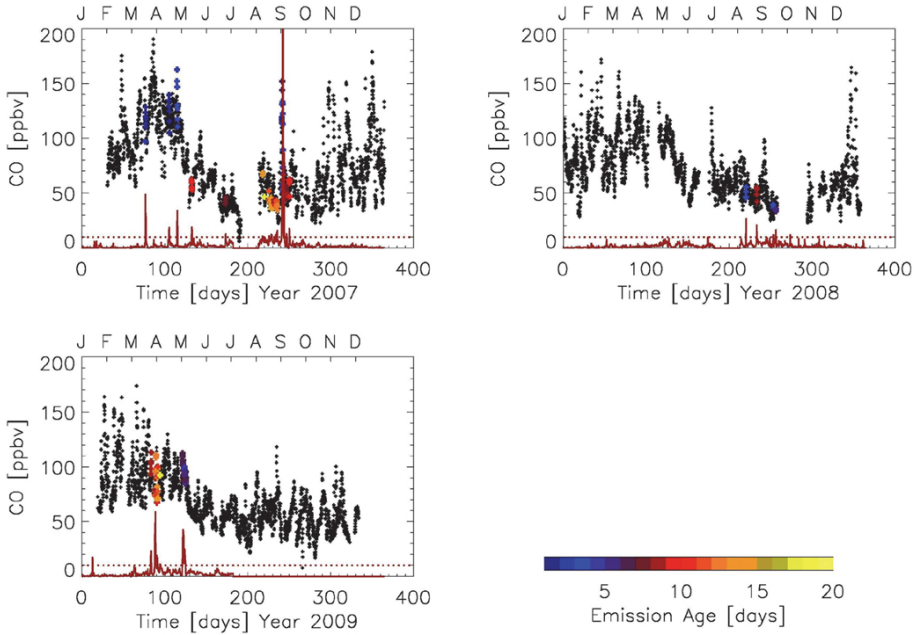

Fig. 3. Time series of observed CO concentration at ICO-OV (black dots) with FLEXPART CO_{fire} (red line). Observations at ICO-OV are tagged with the FLEXPART fire emission age (colour scale) when FLEXPART fire CO exceeded 10 ppb. Observed CO is plotted with a negative constant bias of 30 ppbv to reduce the extent of y-axis.

ACPD
12, 21399–21435, 2012

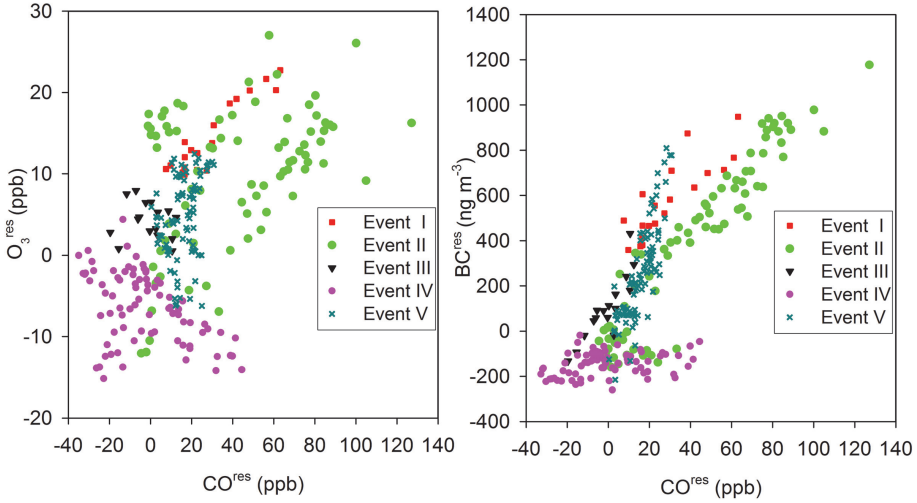

Fig. 4. Relationship between observed CO^{res}, O_3^{res} and BC^{res} during the five major representative BB events listed in Table 1.

ACPD
12, 21399–21435, 2012

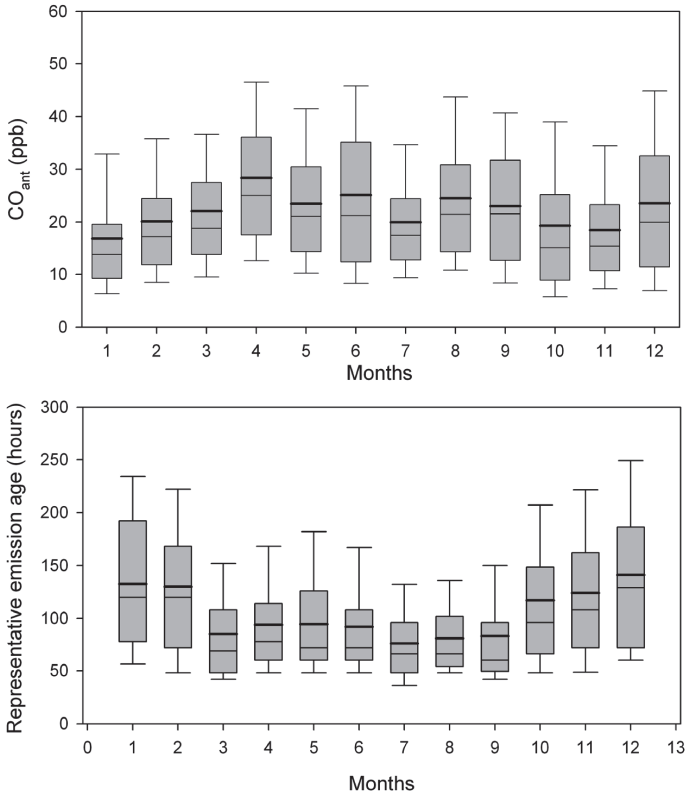

Fig. 5. Monthly distributions of FLEXPART daily CO_{ant} (upper plot) with related representative emission ages (bottom plot) at ICO-OV during the period January 2007–July 2009. The boxes and whiskers denote the 10th, 25th, 50th, 75th and 90th percentiles. Bold lines represent average value. Data at 3-h resolution have been shown.

ACPD
12, 21399–21435, 2012

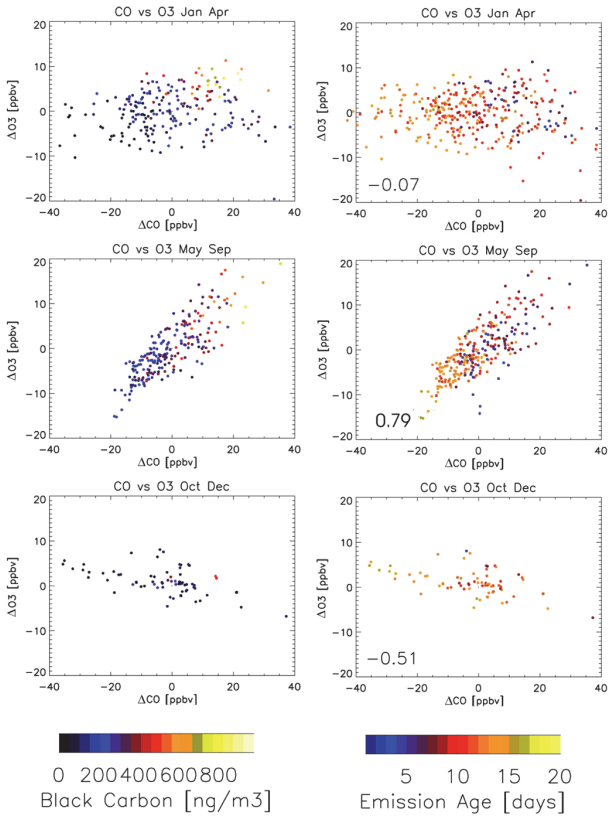

Fig. 6. Observed CO and O_3 anomalies (ΔCO and ΔO_3) for January–April (top), May–September (middle) and October–December (bottom). Left column shows data tagged with BC concentrations observed at ICO-OV, while right column shows data tagged with emission age of CO_{ant} from FLEXPART. Linear correlation coefficients between ΔCO and ΔO_3 (R) are reported for each plot in the left column. Data are averaged over a 24-h time window.

ACPD
12, 21399–21435, 2012

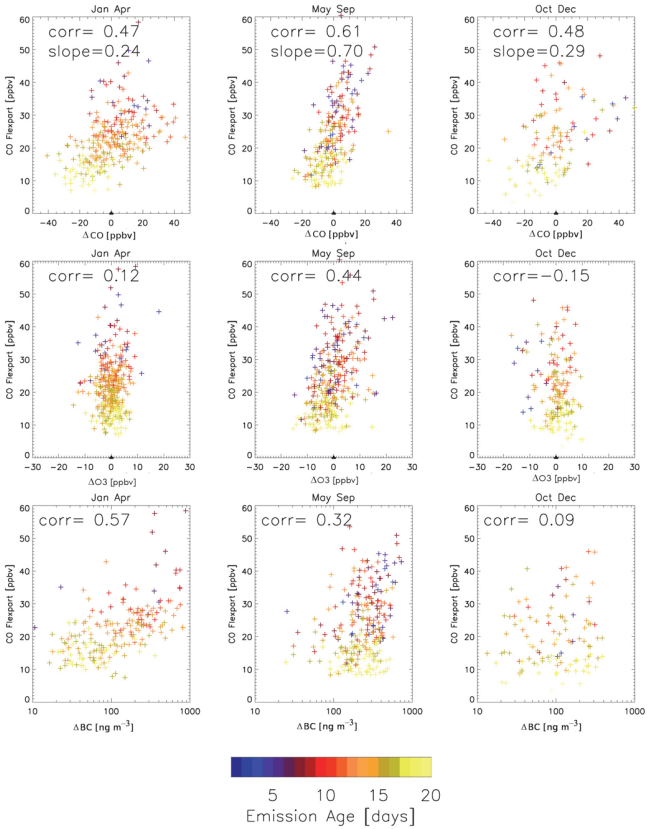

Fig. 7. Observed ΔCO (first row), ΔO_3 (second row) and BC (third row) versus FLEXPART CO_{ant} for January–April (left column), May–September (middle column) and October–December (right column). Data are averaged over 24 h and are tagged with emission age of CO_{ant} (colored scale). The linear correlation coefficients (*corr*) is reported for all the scatterplots while the slope values (*slope*) are only reported for the ΔCO-CO_{ant} correlation.

ACPD
12, 21399–21435, 2012